Nanoscale

PAPER

View Article Online
View Journal | View Issue

Cite this: *Nanoscale*, 2018, **10**, 22612

Curcumin-loaded nanoemulsion: a new safe and effective formulation to prevent tumor reincidence and metastasis†

Simón Guerrero,[a,b,c] Mariela Inostroza-Riquelme,[c,d] Pamela Contreras-Orellana,[a,b,c] Victor Diaz-Garcia,[a,b,c] Pablo Lara,[a,b,c,f] Andrea Vivanco-Palma,[c,d] Areli Cárdenas,[a,c] Victor Miranda,[c,d] Paz Robert,[e] Lisette Leyton, [a,b,c] Marcelo J. Kogan, [c,f] Andrew F. G. Quest*[a,b,c] and Felipe Oyarzun-Ampuero *[c,d]

Curcumin is widely considered beneficial to human health, but insolubility and instability greatly hamper reproducible exploitation of the advantageous traits. Here we report on the development, characterization and evaluation of a curcumin-loaded nanoemulsion (CUR-NEM) that is highly effective in preventing post-surgery tumor reincidence and metastasis. The method of fabrication utilized safe excipients and generated particles of 200 nm (PDI ≤ 0.2) with negative zeta potential (−30 mV) and a high yield of curcumin (95%), which can be converted by lyophilization to a dry powder. *In vitro* assays showed that CUR-NEM is safe in non-cancerous human cells (HEK-293T) and preferentially cytotoxic in gastric (AGS), colon (HT29-ATCC, HT29-US), breast (MDA-MB-231) and melanoma (B16F10) cells. In addition, in melanoma cells the nanoformulation increases intracellular curcumin accumulation and reactive oxygen species (ROS) formation, while preventing cell-migration and invasion. *In vivo* studies in C57BL/6 mice demonstrated that a single dose, applied topically to the wounded area after surgical excision of primary tumors formed upon subcutaneous injection of syngeneic B16F10 cells, was sufficient to completely prevent reincident tumor growth and spontaneous lung metastasis, while in untreated animals 70% reincidence and metastasis were observed. *In vivo* experiments also showed that the fluorescence signal due to curcumin was maintained at least 15 days after topical application of CUR-NEM, while when administered in DMSO the curcumin signal disappeared within 4 days. Importantly, the administration of a dose 22 times larger than that applied topically to animals after tumor surgery did not alter biochemical parameters. Due to the safety and efficacy of the formulation, we envisage it as ideal for topical application in cancer patients following surgery, to prevent tumor reincidence and metastasis. In addition, other routes of administration/protocols could also be proposed to treat/prevent malignant tumors in patients.

Received 31st July 2018,
Accepted 5th November 2018

DOI: 10.1039/c8nr06173d

rsc.li/nanoscale

1. Introduction

Cancer is a group of diseases involving a series of molecular changes to favor uncontrolled cell growth and ultimately to invade (metastasis) other parts of the body. Metastasis, the main cause of deaths in cancer patients, contributes substantially to the current ranking of cancer as the second cause of death worldwide after cardiovascular diseases. Some of the

[a]*Laboratory of Cellular Communication, Program of Cell and Molecular Biology, Institute of Biomedical Sciences (ICBM), Faculty of Medicine, University of Chile, Av. Independencia 1027, Santiago 8380453, Chile*
[b]*Center for Studies on Exercise, Metabolism and Cancer (CEMC), University of Chile, Av. Independencia 1027, Santiago, Chile*
[c]*Advanced Center for Chronic Diseases (ACCDiS), University of Chile, Santos Dumont 964, Independencia, Santiago 8380494, Chile. E-mail: aquest@med.uchile.cl*
[d]*Departamento de Ciencias y Tecnología Farmacéuticas, Facultad de Ciencias Químicas y Farmacéuticas, Universidad de Chile, Santos Dumont 964, Independencia, Santiago 8380494, Chile. E-mail: foyarzuna@ciq.uchile.cl; Tel: +56 229781616*
[e]*Departamento. Ciencia de los Alimentos y Tecnología Química, Facultad de Ciencias Químicas y Farmacéuticas, Universidad de Chile, Casilla 133, Santiago, Chile*
[f]*Departamento de Química Farmacológica y Toxicológica, Facultad de Ciencias Químicas y Farmacéuticas, Universidad de Chile, Santos Dumont 964, Independencia, Santiago, Chile*

†Electronic supplementary information (ESI) available: Electron microscopy image of reconstituted CUR-NEM formulations, UV-Vis spectra of formulations before and after the freeze-drying, cell viability after applying the reconstituted formulations, comparison of the curcumin stability when prepared in DMSO or as CUR-NEM after exposure to UV radiation, and biochemical parameters after applying *in vivo* a dose 22 times larger than those applied in tumor containing animals. See DOI: 10.1039/c8nr06173d

cancers for which the greatest increases in mortality have been observed in recent years include gastric, colon and breast cancer (~20% of increasing between 2005 and 2015).[1] Importantly, melanoma, the most lethal skin cancer type, has increased in prevalence by an alarming 27.2% between 2005 and 2015.[1]

Melanoma is characterized by rapid progression and high resistance to chemotherapy.[2] Additionally, high degrees of invasiveness and metastasis represent the major factors that contribute to poor prognosis and define the outcome for melanoma patients. Approximately 80% of all skin cancer-related deaths are attributed to melanoma and long-term survival of patients is only 5%.[3,4] Despite extensive research efforts, options for the treatment of metastatic disease, beyond invasive surgical interventions, do not exist.[5]

Curcumin (CUR) is a natural compound that possesses a wide range of anti-tumor properties, including the ability to promote cancer cell death, as well as to inhibit angiogenesis.[6] Some studies have shown that CUR is effective against metastasis.[5,7] Additionally, CUR has also been shown to display a favorable safety profile in humans (no dose-limiting toxicity up to 12 g day^{-1}) and several phase I and phase II clinical trials have demonstrated promising effects of oral curcumin administration in patients with colorectal neoplasia, advanced pancreatic and breast cancer.[8,9] More specifically, CUR has also demonstrated anti-melanoma efficacy.[6]

Despite the therapeutic potential of CUR in cancer, its clinical application has been hindered due to a number of limiting characteristics including: rapid metabolism, poor water solubility, instability at neutral pH and upon exposure to light and/or oxygen, and poor uptake by tissues.[10,11] To overcome limitations due to the poor water solubility and low absorption rates, researchers tend to dissolve CUR in organic solvents, like dimethyl sulfoxide (DMSO), prior to evaluation.[12,13] However, DMSO induces severe cell damage and is toxic at many different sites in the body.[14,15]

Nanovehiculization in oil-in-water (O/W) nanoemulsions renders lipophilic molecules soluble in the oil core, while allowing direct administration in biological aqueous fluids.[16] Thus, the advantage of this strategy is that the administration of solvents with topical/systemic toxicity is avoided and CUR is protected against conditions present in the biological environment (neutral pH, oxygen, enzymes and free radicals, *etc.*) known to destabilize CUR.[17,18]

The aim of this study was to encapsulate CUR in O/W nanoemulsions (CUR-NEM) and to test the efficacy and safety *in vitro* and in a preclinical model of melanoma (syngeneic B16F10 cells in C57BL/6 mice). In contrast to other strategies commonly employed to create nanoemulsions containing lipophilic drugs (such as curcumin), our methodology is less contaminating, consumes less energy and can be up-scaled. In top-down approaches, the oil phase is dispersed into homogenous, uniform fine droplets by applying large amounts of energy (50–500 MJ m^{-3}) during the process of emulsification.[19] In contrast, for bottom-up approaches, like the one we propose, the process is designed such that the molecular building blocks assemble into structured systems using less energy.[20,21] Following our approach (solvent displacement), energy is required at the mixing stage as well as during solvent extraction at 40 °C (the solvents can be recovered and used again). The instrumentation required for these procedures, such as mixers and vacuum concentrators are commonly available in industrial facilities. *In vitro* results showed that such nanoformulations were monodispersed, stable and could be converted to a dry powder. Moreover, these preparations were effective and selective at inhibiting proliferation of not only melanoma (B16F10), but also gastric (AGS), colon (HT29-ATCC, HT29-US) and breast (MDA-MB-231) cancer cells. Additionally, administration as CUR-NEM promoted intracellular curcumin accumulation and ROS formation while preventing migration and invasion of B16F10 cells. Importantly, our formulation prolonged curcumin retention at lesion sites (beyond 15 days) and a single dose was remarkably effective at preventing tumor reincidence and lung metastasis post-surgery in a preclinical animal model. Finally, a dose 22 times larger than those applied in animals post-surgery, did not alter biochemical parameters.

2. Experimental

2.1 Materials

Nanoemulsions (NEM): Curcumin (from *Curcuma longa*, C1386, Sigma-Aldrich, USA), Miglyol 812 (neutral oil formed by esters of caprylic and capric fatty acids and glycerol, Sasol GmbH-Germany), Epikuron 145 V (phosphatidylcholine-enriched fraction of soybean lecithin, Cargill-Spain), acetone (Merck-Germany), ethanol (Merck-Germany), Milli-Q water was used as aqueous solvent.

Cell assays: cell medium and antibiotics (RPMI 1640, DMEM-F12, DMEM high glucose, penicillin and streptomycin) were from Gibco-BRL(UK); fetal bovine serum (FBS) was from Biological Industries (US); the 3-(4,5-dimetylthiazol-2-yl)-5-(3-carboxymethoxyphenil)-2-(4-sulfophenyl)-2*H* tetrazolium inner salt (MTS) proliferation assay kit was from Promega (US). 2′,7′-Dichlorofluorescein diacetate (H_2DCFDA) was from Invitrogen (USA).

2.2 Methods

2.2.1 Preparation of curcumin loaded nanoemulsions (CUR-NEM) and content of residual solvents. The method of preparation consists of adding an organic phase containing 125 μL of Miglyol 812 (density 0.945 g mL^{-1}), 30 mg of Epikuron 145 V (phosphatidylcholine-enriched fraction of soybean lecithin), 2.76 mg of curcumin, 0.5 mL of ethanol and 9.5 mL of acetone; to an aqueous phase containing only Milli-Q water (20 mL). The above solution was rotaevaporated until a volume of 5 mL remained in order to eliminate the organic solvents from the mixture (ethanol and acetone) as well as to concentrate the curcumin. The formation of the nanoemulsions was instantaneous and spontaneous, as evidenced by the

milky appearance of the mixture. Residual solvents were detected following the USP 32 of the US pharmacopeia ⟨467⟩ guidelines on an Agilent GC-FID 5890 using a DB-624 column (length 30 m × 0.32 mm of internal diameter × 0.25 um of wall thickness) applying the following temperature program: initially at 40 °C for 10 min, followed by a gradient of 10 °C min^{-1} up to 250 °C, with the injector at 200 °C and the detector at 250 °C.

2.2.2 Physicochemical characterization of the nanocarriers. The size and zeta potential of the colloidal systems were determined by photon correlation spectroscopy and laser Doppler anemometry, with a Zetasizer Nano-ZS (Malvern Instruments, UK). Scanning transmission electron microscopy (STEM, FEI Inspect 50-USA) images were obtained to analyze the morphology of the carriers. STEM images were obtained by sticking a droplet (10 μL) of the nanoparticle suspension (fresh or lyophilized and reconstituted) to a copper grid (200 mesh, covered with Formvar) for 2 min, then removing the droplet with filter paper avoiding the paper touching the grid, then washing the grid twice with a droplet of Milli-Q water for 1 min and removing the droplet with filter paper. Later, the sample was stained with a solution of 1% phosphotungstic acid by adding a droplet of this solution to the grid for 2 min and subsequently removing the droplet with filter paper. Finally, the grid was allowed to dry for at least 1 h before analysis.

2.2.3 Association efficiency in the nanocarriers. The Association efficiency of curcumin in the nanocarriers was determined by analyzing the difference between the total amount of curcumin in the formulation and the free curcumin recovered after an aliquot of the sample was isolated using Vivaspin® tubes (8500G, 20 min, MWCO 100 kDa). The yield of curcumin in the formulation was determined by analyzing the difference between the total amount of added curcumin and the amount obtained after the elaboration process. Free curcumin and bulk CUR-NEM samples (200 μL) were mixed with acetone (400 μL), stirred in a vortex (1 min) and then curcumin was analyzed by HPLC as described by Jayaprakasha *et al.* (2002).[22] The HPLC system included a Merck Hitachi L-6200 pump, a Waters 996 photodiode-array detector and a C18 column (5μm, 4.6 i.d. 250 mm, PerkinElmer). The mobile phase consisted of methanol (A), 2% acetic acid (B), and acetonitrile (C). Quantitative levels of curcuminoids were determined using the above solvents programmed linearly from 45 to 65% acetonitrile in B for 0–15 min. The gradient then went from 65 to 45% acetonitrile in B for 15–20 min, with a constant of 5% A. The flow rate was 1.0 mL min^{-1}. Curcuminoids were quantified using a calibration curve of curcumin (0.004–0.08 mg mL^{-1}, R^2 = 0.999) and the detection was at 425 nm.

2.2.4 Curcumin loading in the nanocarriers. The final curcumin loading (% w/w) was calculated by dividing the amount of curcumin associated with the nanoemulsion by the total weight of the nanoemulsions. For the calculation of the total weight of the nanoemulsions, 5 mL of the formulation were lyophilized in glass vials, which were weighed before adding the formulation and after freeze drying to assess the total solid mass (glass vials + formulation).

2.2.5 Freeze-drying and reconstitution studies of curcumin loaded nanoemulsions. Concentrations of NEM (0.5 and 1% w/v) loaded with CUR and the cryoprotectant trehalose (5% and 10%) were considered as the variables for the lyophilization study, following a procedure similar to the one previously described by our group.[16] Briefly, 2 mL of the nanocarriers were freeze-dried and 2 mL of Milli-Q water were used to reconstitute the formulation. Then, 20 μL of the reconstituted formulation were diluted with Milli-Q water until 1 mL, and size was measured.

The UV-vis spectra of CUR from fresh formulations and the freeze-dried preparations reconstituted in water were evaluated in quartz vessels and scanned at wavelengths ranging from 350 to 550 nm (Lambda 25, PerkinElmer-USA). For analysis, aliquots (200 μL–400 μL) of CUR-NEM, either freshly prepared or freeze dried and reconstituted in acetone (final volume 5 mL) were vigorously mixed in a vortex. Then the formulations were centrifuged for 30 min at 12 000*g* (Hermle Labortechnik, Germany) and the supernatant was analyzed in the spectrophotometer.

2.2.6 Cell culture conditions. Metastatic murine melanoma cells (B16F10, ATCC) and human gastric adenocarcinoma (AGS, ATCC) were cultured in RPMI 1640 (GIBCO) supplemented with 10% FBS (Biological Industries) and antibiotics (100 U mL^{-1} penicillin and 100 μg mL^{-1} streptomycin, GIBCO) as described Urra H. *et al.*[23] Human breast cancer cells (MDA-MB-231, ATCC) were cultured in DMEM-F12 (GIBCO) containing 10% FBS (Biological Industries) and antibiotics (100 U mL^{-1} penicillin and 100 μg mL^{-1} streptomycin, GIBCO) as described Urra H. *et al.*[23] Human embryonic kidney cells (HEK293T, ATCC), human colon adenocarcinoma (HT29, ATCC) and metastasis-derived human colon adenocarcinoma (HT29, US) cell lines, were cultured in DMEM high glucose medium (GIBCO) containing 10% FBS (Biological Industries) and antibiotics (100 U mL^{-1} penicillin and 100 μg mL^{-1} streptomycin, GIBCO) as described Torres *et al.*[24] Cells were cultured at 37 °C and 5% CO_2.

2.2.7 Viability assays. Cells were seeded in 96-well plates at a density of 1×10^4 cells per well and incubated for 24 h in culture medium. Then, cells were treated for another 24 h with formulations (10 μL). Cell proliferation was evaluated removing curcumin treatments and replacing with fresh culture medium containing 10% of tetrazolium compound of MTS® assay (CellTiter 96® Aqueous Non-Radioactive Cell Proliferation Assay), according to the manufacturer's (Promega, Madison, WI). The soluble formazan produced by live cells is detected as absorbance at 490 nm on a Multiscan Reader (Synergy-H4, Biotek), as described previously Adura *et al.*[25] Background values contributed by excess cell debris and bubbles obtained by measuring at 650 nm were subtracted.

2.2.8 Reactive oxygen species (ROS) determination by FACS. Cells were seeded in 24-well plates at a density of 4×10^4 cells per well and incubated for 24 h in culture medium. Then, cells were treated with 12.5 μM of curcumin containing

vehicles or empty vehicles (50 μL) for another 24 h. Finally, cells and medium were recovered. ROS production was evaluated employing 2′,7′-dichlorofluorescein diacetate (H_2DCFDA-0.1 μM) as described by Chang *et al.*[26]

2.2.9 Confocal fluorescence microscopy. Cells were seeded in 24-well plates at a density of 4×10^4 cells, on sterile coverslips (12 mm round coverslips glasses-Deckglässer), and grown for 24 h in complete medium. Then, cells were treated with vehicles containing 12.5 μM of curcumin or empty vehicles (50 μL) for another 24 h. Cells were subsequently washed with ice-cold PBS and fixed with 4% paraformaldehyde for 10 min. Afterwards, they were washed three times with buffer containing 50 mM Tris-HCl (pH 7.6), 0.15 M NaCl and 0.1% sodium azide (Universal buffer). Later, cells were permeabilized with 0.1% Triton™ X-100 (Sigma-Aldrich) in Universal Buffer for 10 min, washed twice with the same buffer and then blocked with 2% bovine serum albumin. Cells were stained then labeled with anti-EEA1 followed by secondary antibodies coupled to Alexa[488]. DAPI was used to stain nuclei as described.[23] Coverslips were mounted on a glass slide using Fluoromount G® Mounting Medium (Southern Biotechnology Associates, USA) and sealed. Confocal images were acquired on a Zeiss LSM700 microscope (Zeiss, NY, USA) with a 63×/1.3 Imm Corr DIC objective for water or glycerine immersion with a pinhole of 70 μm. The images were analyzed using the software ImageJ and Imaris.

2.2.10 Flow cytometry. Cells were seeded in 24-well plates at a density of 4×10^4 cells per well and incubated for 24 h. Afterwards, cells were exposed to vehicles containing 12.5 μM of curcumin or empty vehicles (50 μL) for another 24 h. Then, cells and cell medium were recovered in borosilicate glass tubes, centrifuged to remove trypsin with PBS and resuspended in FACS buffer (PBS with 1% serum and 5 mM EDTA). The mean relative fluorescence of cell populations from the different treatment groups was determined and reported as mean ± standard deviation of values from three independent experiments.

2.2.11 Curcumin photo stability following UV exposure. Curcumin solutions/suspensions were prepared in acetone, DMSO or as CUR-NEM. Then each solution/suspension was transferred to a 5 mL double-wall cell, light-protected by black paint, but with a small window at the center that permits sample irradiation. Circulating water maintained the cell temperature at 20 ± 0.5 °C. Samples were irradiated with a Hg high power UV lamp at 254 nm. Subsequently, the samples were analyzed by measuring their absorbance at 424 nm.

2.2.12 Transwell migration assays. Prior to experiments, the bottom side of each Boyden Chamber insert (transwell costar, 6.5 mm diameter, 8 μm pore size) was coated with 2 μg mL^{-1} fibronectin. B16F10 cells (5×10^4) previously treated 24 h with CUR-NEM, CUR and controls, were resuspended in serum-free medium and added to the top chamber of the insert, while serum-free medium was added to the bottom chamber. After 2 h, inserts were removed, washed, and cells that had migrated to the lower side of the inserts were stained with 0.1% crystal violet in 2% ethanol and counted in a microscope as previously described.[23]

2.2.13 Matrigel invasion assay. B16F10 cells (5×10^4) were seeded, allowed to grow for 24 h, and treated with CUR-NEM, CUR-DMSO or the respective controls. Then, serum-starved cells (2×10^5) were seeded (24 h) over 8 μm-porous inserts covered with Matrigel (Matrigel Invasion Chamber 8.0 lm; BD Biosciences, Bedford, MA, USA). Inserts were fixed in cold methanol and stained with 0.5% toluidine blue in 2% Na_2CO_3. The membranes were mounted in Mowiol, and observed under a light microscope. At least 10 fields were evaluated (at 40× magnification) to determine the number of cells per field.

2.2.14 Animal studies. C57BL/6 mice were obtained from the Instituto de Salud Publica (Santiago, Chile) and housed in the animal facility of the Centro de estudios en Ejercicio, Metabolismo y Cancer (Instituto de Ciencias Biomedicas, Universidad de Chile). Mice between 8 and 12 weeks of age and average weight of 25 g were used for experiments. All animal procedures were performed in accordance with the Guidelines for Care and Use of Laboratory Animals of University of Chile and approved by the local bioethics Committee (CBA#889).

Reincident tumor growth and lung metastasis in animal models. Subcutaneous tumor growth (B16F10 cells) and metastasis assays (B16F10 cells) in C57BL/6 mice studies were developed as we previously described.[27] A single dose of CUR-NEM (1500 μM) or controls (NEM and physiological serum) were administered after excising the tumor and before suturing the wound. Volumes to be employed were calculated by correlating tumor volumes with those used for *in vitro* cell viability studies. For example, *in vitro* 10 μL of CUR-NEM was administered to each well (0.3 cm^2 per well considering plates of 96 wells). Thus, if the area of a tumor was on average 2.5 cm^2 the volume of CUR-NEM added post-surgery was 83.3 μL (2.5 cm^2/0.3 cm^2 × 10 μL).

In vivo fluorescence detection. A single dose of the treatments (CUR-NEM and CUR-DMSO, 1500 μM) and the negative control (0.9% NaCl) were administered after excising the tumor and before suturing the wound (for identifying administered volumes see in the section "Reincident tumor growth and lung metastasis in animal models"). Animals were maintained for 15 days. At different time intervals (first day at 2, 4, 8, and 24 h; then once a day up to 15 days), the mice were anaesthetized for 5–15 min (2.5% isoflurane in O_2) and imaged by fluorescence using the imaging system *In vivo* FX PRO (excitation 430 nm/emission 540 nm, Bruker, USA). Fluorescence in regions of interest (ROI) for each experiment was quantified on images obtained by molecular imaging Bruker software (USA).[28,29]

Acute toxicological assay. The animals were 6 weeks of age and between 19.9 and 21.2 grams in weight at the start of the trial. All test results for microbiological and viral pathogens were negative, prior to initiating the trial (Smart Spot, South Africa). On the day of surgery, a maximum volume of 300 μL of the curcumin nanoemulsion (concentration of 0.01 M of curcumin, thus a dose 22 times higher than the one applied to

animals) was applied to the area of tumor growth post-surgery in the animal model. Day 14 post-surgery, animals were euthanised. Then, all blood components were checked by EPOC blood analysis (BGEM test cards, Epocal, Canada).

2.2.15 Statistical analysis. All data were displayed as mean ± standard error of mean (SEM) of three independent experiments using the GraphPad Prism 5.03 program (GraphPad software, Inc.). Data were analyzed by one-way ANOVA followed by Tukey multicomparison tests for *in vitro* assays or a non-parametric Mann–Whitney test in the case of *in vivo* assays. Statistical significance was determined at the 95% confidence interval.

3. Results and discussion

NEM were prepared following the solvent displacement method. This strategy has been exploited to create vehicles loaded with cytotoxic drugs (docetaxel and plitidepsin) and coated with different polymers (nanocapsules) to improve the drug efficacy after intravenous administration.[16,30–33] In the present study, we focused on working with the non-cytotoxic compound curcumin, which has been shown to be quite effective in the treatment of a variety of cancers[6,8,9] but is limited in its applications due characteristics like rapid metabolism, poor water solubility, instability at neutral pH and upon exposure to light and/or oxygen, as well as poor uptake by tissues.[10,11] These same characteristics are also largely responsible for the great variations in experimental outcomes reported in the literature using curcumin. For this reason, we chose to develop a nanoformulation that would render CUR soluble and at the same time protect the molecule. Additionally, considering that we envisioned applying the formulation topically in the wounded area after surgical removal of primary tumors (to prevent/treat reincident tumor growth and metastasis from remnant cancer cells), we avoided the use of polymers as coating material, in order to simplify elaboration procedures (less components), reduce production time by avoiding additional incubation steps, and consequently, lowering costs. Additionally, the presence of further components (*i.e.* polymer) can induce higher metabolic stress in the recipient tissue, producing detritus and blocking an adequate oxygenation. This could impair the wound closure, adversely affecting the surrounding healthy tissue and promoting the growth of microorganisms.[34,35] The elaboration method involved the addition of an organic phase including CUR (acetone, ethanol, the oil Miglyol, and the natural surfactant Epikuron) to water and then extracting the organic solvents (until ethanol and acetone presence was lower than 5 ppm) by rotaevaporation (see scheme in Fig. 1).[16] This strategy permits obtaining nanocarriers in the range of 195–217 nm, (PDI ≤ 0.2), with a negative zeta potential (−30 to −36 mV). Importantly, the yield of CUR in the formulation was efficient (95%), reaching a level of drug loading of 2.1 ± 0.1%. Characterization by electron microscopy revealed such nanocarriers to be round and highly regular in shape (Fig. 1), which is in agreement with the size-data obtained by dynamic light scattering (≈200 nm).

Freeze-drying (lyophilization) is one of the most frequent and efficient methods to maintain the properties of nanoparticle suspensions during storage over extended periods of time. This strategy, due to the total elimination of water, prevents the contamination by microorganisms while facilitating the transportation due to the lower weight of the final product.[16] The size, zeta potential and shape (electron microscopy images) of CUR-NEM upon reconstitution of the freeze-dried product were studied[16] (Fig. 1 and Fig. S1†). Overall the results indicate that optimal reconstitution of the dried product was achieved without altering the size, zeta potential and shape of the original (fresh) CUR-NEM. Indeed, the spectrum of CUR was similar for fresh CUR-NEM and for the reconstituted lyophilized formulations (see Fig. S2 in ESI†).

Cell viability following treatment with formulation were assessed in several cell lines representative of important types of cancer worldwide (AGS: human gastric adenocarcinoma; HT29 ATCC: colorectal adenocarcinoma; HT29 US: cells derived from HT29(ATCC) with elevated metastatic potential; MDA-MB-231: human mammary gland adenocarcinoma and B16F10: murine melanoma) and compared with the effects

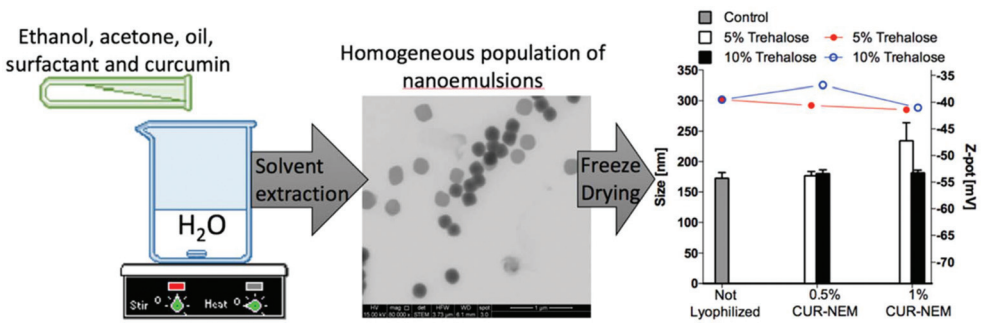

Fig. 1 Preparation and characterization of curcumin (CUR)-loaded nanoemulsions: elaboration scheme (left), electron microscopy images of resulting nanoemulsions (center), stability of formulations before and after being converted to a dry powder (right, bars represent the size of the formulations while lines represent the zeta potential).

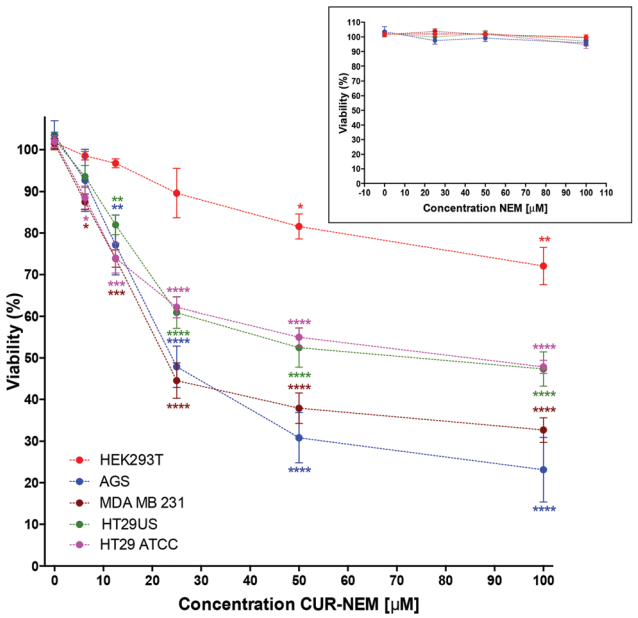

Fig. 2 Viability of different human cancerous cell lines: viability was evaluated using the MTS assay in the non-cancerous cell line (HEK 293T), and the cancer cell lines (AGS, MDA-MB-231, HT29 ATCC, and HT29 US) after treatment with CUR-NEM for 24 h. Insert graph shows the results for treatment with different concentrations of NEM (n = 3, $^{**}P < 0.01$; $^{***}P < 0.001$; $^{****}P < 0.0001$).

observed in the non-cancerous cell line HEK-293T (human embryonic kidney). As shown in Fig. 2, all cancer cells tested were sensitive to CUR-NEM. The observed IC_{50} values were 24 ± 6.1 μM for AGS, 26.2 ± 3.5 μM for MDA-MB-231, 75.7 ± 5.4 μM for HT29 US and 84.6 ± 3.3 μM for HT29 ATCC cells. As evidenced in the figure, the non-cancerous cell line (HEK-293T) was only slightly affected and ~80% of the cells remained viable after the highest dose of the formulation was administered. As shown in the same figure, the NEM vehicles (blank nanoemulsions) did not affect cell-viability, indicating the safeness of the formulation.

Cell viability was also assessed in the B16F10 melanoma cells following treatment with CUR-NEM. These cells were selected because, in addition to being highly resistant, proliferative and metastatic,[36] they are suitable cells to study *in vivo* in syngeneic C57BL/6 mice (with a functional immune system) tumor formation after subcutaneous injection, as well as reincident tumor growth and metastasis after the primary tumor has been surgically removed,[27,37] which represented an important objective in this study. As shown (Fig. 3(a)), the NEM vehicles (blank nanoemulsions) did not affect cell-viability. Importantly, the results also indicate that CUR-NEM were as efficient in decreasing proliferation as curcumin dissolved in the solvent DMSO (IC_{50} = 46.0 ± 5.8 μM and 34.8 ± 7.5 μM, respectively). However, it is well established that DMSO is toxic.[14,15] We also demonstrated in viability assays that the formulation maintained a similar level of activity after the lyophilization process (see Fig. S3 in ESI†). To the best of our knowledge, there is only one other study available in which the cytotoxicity in B16F10 cells was evaluated after administering CUR in nanoemulsions.[38] This proposal is different from ours because the authors selected a procedure that involves the use of chloroform and requires high energy

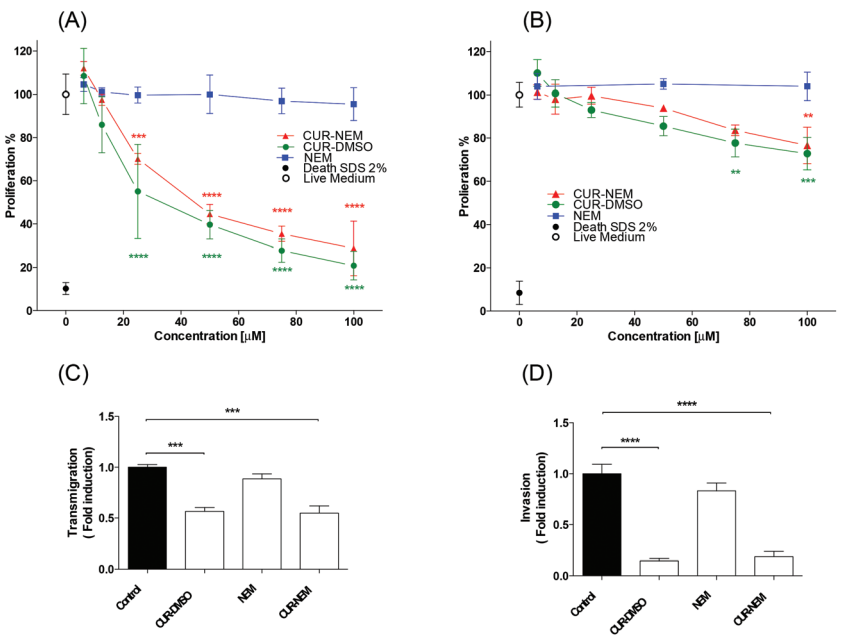

Fig. 3 Viability, cell migration and cell invasion after applying the formulations: viability evaluated using the MTS assay in B16F10 (a) and HEK 293 cells (b) after treatment with CUR-DMSO, NEM or CUR-NEM for 24 h (n = 3, $^{**}P < 0.01$; $^{***}P < 0.001$; $^{****}P < 0.0001$). Effects on B16F10 cell migration (c) and invasion (d) of NEM and CUR containing formulations (12.5 μM of CUR). Cells were preincubated for 24 h (n = 3, $^{***}P < 0.001$; $^{****}P < 0.0001$).

to be applied (vigorous mixing and sonication) to obtain NEM in the range of 50–70 nm. Unfortunately, those results (IC_{50} of 8.2 m μg mL^{-1} or 22.2 μM) are not easily comparable with ours because the experiments were done using different formulations and experimental conditions such as culture medium and time of exposure to the formulations (48 h compared with 24 h in our experiments). Cell viability was also evaluated following treatment of the non-cancerous cell line HEK-293T (human – embryonic kidney). At the highest doses tested, CUR-NEM diminished viability of these cells by only ≈25% similarly to the formulation containing DMSO (Fig. 3(b)).

CUR treatment has been shown to reduce migration and invasion of cancer cells.[39–46] This effect was attributed to alterations in several signaling pathways. For instance, in Hca-F cells this effect was linked to alterations in caveolin-1 (Cav-1) and EGFR mediated signaling pathways.[40] In addition, in a variety of cell lines (GBM, NCI-H446, NCI-1688, SK-Hep-1 and CAFs) the reduction in migration and invasion was explained because curcumin inhibits the JAK2/STAT3 signaling pathway.[39,41–46] Additionally, in A549 cells CUR has been shown to down-regulate plectin expression, a protein that participates in cytoskeleton organization and plays an important role in migration and invasion.[41,47] CUR has also been shown to inhibit the matrix metalloproteinases (MMP)-2 and 9, as well as VEGF in A549, SK-Hep-1 and MCF-7 cells.[44,47,48] Of note, MMPs are important during metastasis.[41,44,49] In this study, we wondered if these beneficial characteristics were maintained if curcumin was included in the nanoemulsion (CUR-NEM). Indeed, migration of B16F10 cells was substantially decreased (≈50%) upon cell preincubation with either CUR-NEM or CUR-DMSO, while blank nanoemulsions (NEM) did not lead to any significant effects (Fig. 3(c)). Moreover, a highly significant 10-fold reduction in the invasiveness was detected following treatment with either CUR-NEM or CUR-DMSO, while NEM alone had no significant effects (Fig. 3(d)). Similar results were obtained previously by Wang *et al.*,[40] who observed that CUR-DMSO reduced migration 3-fold and invasion 7-fold in the hepatoma cell line Hca-F. Importantly, our nanoformulation is shown here to maintain the beneficial effects of CUR to the same extent as reported for CUR-DMSO, but without the necessity of employing the toxic solvent DMSO.

CUR has also been demonstrated to specifically increase ROS in cancer cells.[50] This report contradicts, to some extent, the findings of others showing that CUR specifically binds to the TrxR receptor,[51] and also multiple enzymes involved in ROS-metabolism (CBR1, GSTP1, AKR1C1, GLO1, NQO1, among others).[44,50–59] Also, Larasati *et al.* demonstrated that CUR binds to several enzymes involved in ROS metabolism,

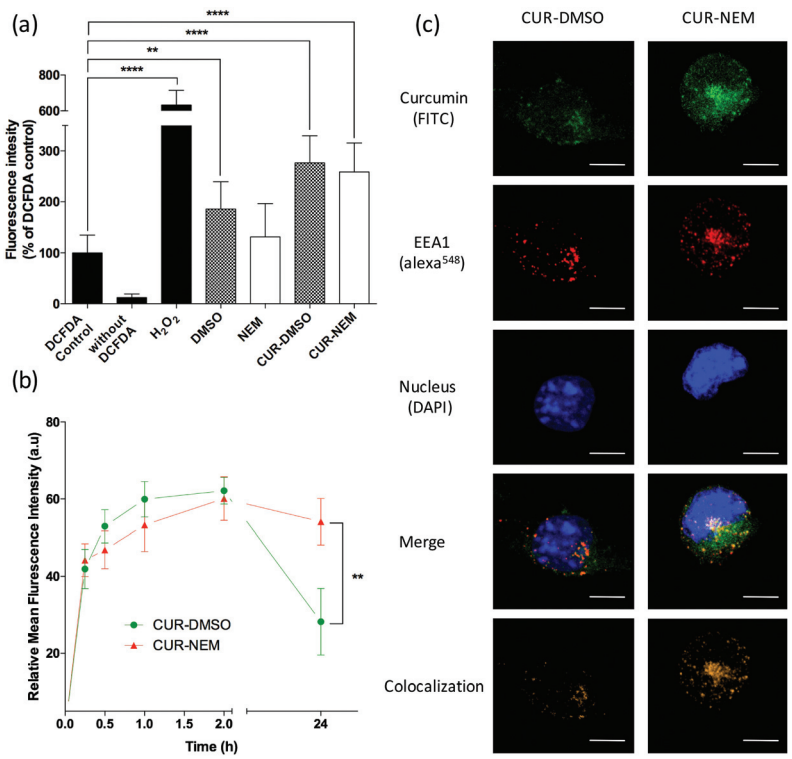

Fig. 4 ROS levels, flow cytometry analysis and confocal images after applying the formulations: (a) ROS levels after incubation of B16F10 cells with DMSO, NEM, CUR-DMSO or CUR-NEM for 24 h (CUR containing formulations had 12.5 μM of CUR) (n = 3, $^{**}P < 0.01$; $^{***}P < 0.001$; $^{****}P < 0.0001$). (b) Flow cytometry analysis after incubating B16F10 cells with CUR-NEM and CUR-DMSO (12.5 μM of CUR) preparations for increasing periods of time (0.25, 0.5, 1, 2 and 24 h) (n = 3, $^{**}P < 0.01$). (c) Confocal images after 24 h of incubation with B16F10 cells (scale bars: 10 μm).

thereby regulating intracellular ROS levels, which trigger p53-dependent and -independent checkpoint pathways, resulting in apoptosis or senescence.[59] With this in mind, we evaluated if ROS increased in melanoma cells (B16F10) following administration of CUR-NEM. As evidenced in Fig. 4(a), all formulations containing CUR (CUR-NEM and CUR-DMSO) increased ROS levels 2-fold at a dose of 12.5 μM of CUR. Importantly, the solvent DMSO alone, significantly increased the basal ROS levels, while this was not the case for the NEM controls. This increase in ROS likely contributes, at least in part, to the DMSO toxicity observed in several studies.

In order to complement the *in vitro* results, we considered it important to determine if the formulation permitted the interaction with and then internalization of CUR into melanoma cells. As eluded to above, many of the anticancer effects attributed to CUR are related to intracellular phenomena. Flow cytometry (FACS) assays indicated that CUR-NEM was rapidly and efficiently taken up by melanoma cells. Indeed, CUR levels in cells after 2 and 24 h of exposure to CUR-NEM, increased by only 36% and 22% respectively, compared to values obtained after 15 min (Fig. 4(b)). Interestingly, while cell-associated CUR levels were similar initially for CUR-NEM and CUR-DMSO formulations (until 2 h), these levels remained similar after 24 h only for CUR-NEM, but decreased by 55% in CUR-DMSO treated cells. This result suggests that encapsulation of CUR in NEM is protective. As suspected, based on the previous results (uptake by FACS), confocal microscopy experiments revealed higher levels of CUR inside cells (after 24 h) when added as CUR-NEM compared with CUR-DMSO treated cells (Fig. 4(c)), again suggesting that CUR is stabilized in the nanoemulsions. In addition, experiments evaluating the stability of curcumin in CUR-NEM and CUR-DMSO revealed greater protection against UV exposure in the nanovehicle (see Fig. S4 in ESI†). As shown in Fig. 4(c), there was a significant increase in the colocalization between CUR-NEM and EEA1 (antibody against early endosome antigen 1), compared with CUR-DMSO, indicating that the endosomal entry route is favored by using our formulation.

Interestingly, internalization occurred despite the negative NEM zeta potential of −30 to −36 mV. As described in several papers, the presence of negative charge on the surface of O/W nanoemulsions and O/W nanocapsules (zeta potential from −16 to −52 mV) does not appear to generate a problem either for emulsion/capsule uptake, access to intracellular compartments or the improvement of drug action at such intracellular sites.[16,60–63] In an interesting paper, Calvo *et al.* (1996)[60] describe the cellular internalization of nanoemulsions of 220 nm and −42 mV (our formulation have 200 nm and −30 mV). In that paper, authors sustained that the size, instead of charge (compared negatively and positively charged O/W nanocarriers), is critical. In our case, intracellular access may also be facilitated by the colloidal size of the NEM[60] and the inherent permeability enhancing properties of phospholipids (main component of the surfactant, Epikuron 145 V).[64]

Extirpation of primary tumors represents one of the principle clinical approaches employed to control tumor malignances. Usually, the extracted cells are then subjected to biochemical and histological analysis, in order to identify whether cells are cancerous or not. Unfortunately, in those cases where cancer cells are detected, the risk of tumor reincidence at the same site and metastasis to distant tissues is elevated. With this in mind, our approach was to apply the CUR-NEM formulation after surgical removal of the primary tumor to prevent/treat reincident tumor growth and metastasis in remnant cancer cells.

The *in vivo* experiments (preclinical animal model) show that the administration of only one dose of CUR-NEM, to the wounded area after surgical removal of tumors, completely prevented tumor reincidence (Fig. 5(a)). Additionally, this single dose of CUR-NEM completely abolished lung metastasis (Fig. 5(b)). In both cases, untreated animals showed 70% of tumor reincidence and metastasis. These results are very promising because melanoma cells are very aggressive and represent a type of cancer with very high mortality rates.[1–5,65–67] To the best of our knowledge, this is the first study showing that topical application of a formulation is sufficient to

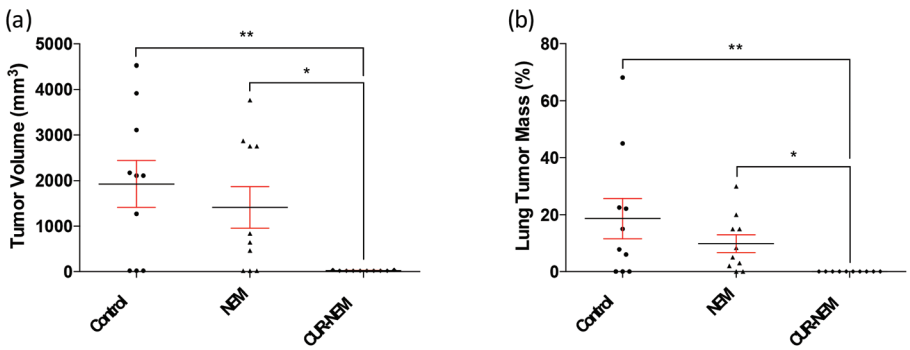

Fig. 5 Tumor reincidence (a) and metastasis (b) in a pre-clinical mouse model. B16F10 cells were injected sub-cutaneously into C57BL/6 mice and tumors were allowed to develop for 14 days prior to surgical removal as described. The resulting wounded zone post-surgery was either not treated (control), treated with NEM or with CUR-NEM. Mice were then sacrificed 21 days post-surgery and tumor growth at the initial site (a) as well as lung tumor mass (b) were evaluated as described. (n = 10, *P < 0.05; **P < 0.01).

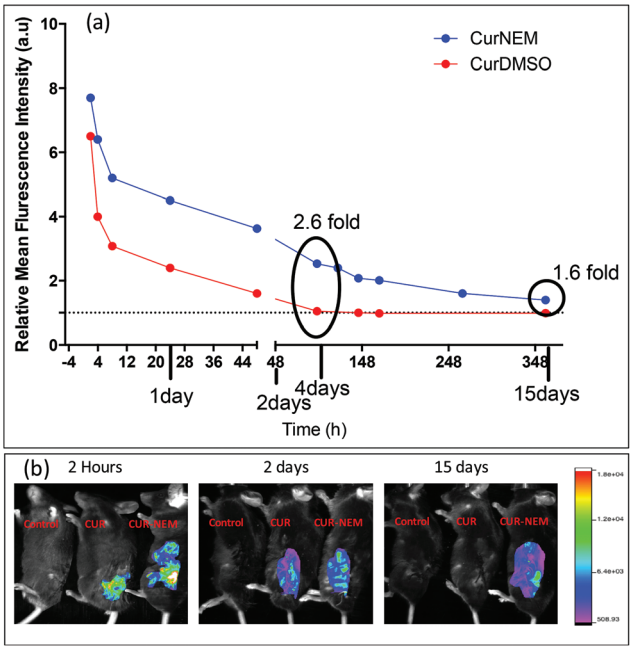

Fig. 6 Curcumin fluorescence observed after tumor excision and CUR-NEM treatment; (a) graph showing the fluorescence quantification and summarizing the ROI values observed *in vivo* at the different time points; (b) images showing the fluorescence of anesthetized mice at 3 different times (after 2 hours, 2 days and 15 days).

prevent tumor reincidence and metastasis from remnant cancer cells after the primary tumor has been excised.

In order to obtain evidence for the protective role of NEM, we tracked the fluorescence signal of curcumin administered as CUR-NEM and compared with that of CUR dissolved in DMSO. Fig. 6 shows that the fluorescence signal following CUR-NEM application to the site of surgery remains detectable for at least for 15 days, while CUR dissolved in DMSO was no longer detectable after day 4. These results concur with those obtained by FACS, confocal microscopy, and photo stability, indicating that CUR was better protected in NEM than when administered in DMSO. Such extended presence of CUR at the site of application may explain the observed protection against reincident tumor growth and metastasis. Finally, to determine whether acute toxicological responses are observed following use of the formulation, a dose 22-times larger than the one applied in the pre-clinical experiments, was also evaluated in animals. As shown in Tables S1, S2 and S3 (see in ESI†), all biochemical parameters tested remained normal. These results confirm the safety of our formulation even at significantly higher doses than those administered in the preclinical animal model.

4. Conclusions

High degrees of invasiveness and metastasis represent the major factors that contribute to poor prognosis and detrimental outcome for cancer patients. As described, here we report on the development, characterization and evaluation of a nanoformulation containing CUR for the treatment of reincident tumor growth and metastasis. This nanoemulsion is easy to prepare and can be converted into a dry powder with no loss in effectivity upon reconstitution. *In vitro*, this nanoformulation preferentially reduced proliferation in cancer cells rather than in non-cancerous cells. Also, CUR-NEM preparations increased ROS levels and permitted more persistent intracellular accumulation of CUR, while preventing migration and invasion of melanoma cells. Considering that our nanoformulation eliminates the use of toxic solvents and employs with FDA-approved excipients, we envisage this preparation as highly suitable for pre-clinical/clinical therapy. In this sense, we demonstrate *in vivo* that a single dose of this formulation, applied topically in the area of the excised primary tumor, was sufficient to prevent melanoma reincidence and lung metastasis post-surgery from remnant cells. *In vivo* experiments also show that the fluorescence signal of curcumin was maintained over 15 days after applying topically the nanoformulation, which is significantly longer than when curcumin was administered in DMSO (4 days). Importantly, the administration of a dose 22 times larger than those applied in tumor containing animals did not alter biochemical parameters.

In summary, we consider the exceptional benefits of this formulation make it an ideal product to be tested topically in human patients following melanoma surgery (and surgery of other malignant tumors), to prevent tumor reincidence and metastasis. In addition, other routes of administration/protocols could also be proposed to treat/prevent malignant tumor growth in patients.

Conflicts of interest

There are no conflicts to declare.

Acknowledgements

This work was supported by FONDECYT 1161450 (F. O.-A.), FONDEQUIP EQM160157 (F. O.-A.), FONDEQUIP EQM170111 (F. O.-A.) FONDECYT 1130250, 1170925 (A. F. G. Q.), Anillo ACT 1111 (A. F. G. Q.), FONDECYT 1150744 (L. L.), CONICYT-FONDAP 15130011 (A. F. G. Q., M. K., F. O.-A., L. L.), CONICYT post-doctoral award 3140463 (S. G.) and CONICYT PhD fellowships awards 21120816 (V. D.-G.), 21140353 (P. L.), 21141137 (M. I.-R.).

Notes and references

1 H. Wang *et al.*, *Lancet*, 2016, **388**, 1459–1544.
2 C. Karimkhani, R. Gonzalez and R. P. Dellavalle, *Am. J. Clin. Dermatol.*, 2014, **15**, 323–337.
3 T. L. Hocker, M. K. Singh and H. Tsao, *J. Invest. Dermatol.*, 2008, **128**, 2575–2595.

4 J. Ferlay, I. Soerjomataram, R. Dikshit, S. Eser, C. Mathers, M. Rebelo, D. M. Parkin, D. Forman and F. Bray, *Int. J. Cancer*, 2015, **136**, E359–E386.
5 L. G. Menon, R. Kuttan and G. Kuttan, *Cancer Lett.*, 1999, **141**, 159–165.
6 P. Anand, C. Sundaram, S. Jhurani, A. B. Kunnumakkara and B. B. Aggarwal, *Cancer Lett.*, 2008, **267**, 133–164.
7 L. G. Menon, R. Kuttan and G. Kuttan, *Cancer Lett.*, 1995, **95**, 221–225.
8 R. E. Carroll, R. V. Benya, D. K. Turgeon, S. Vareed, M. Neuman, L. Rodriguez, M. Kakarala, P. M. Carpenter, C. McLaren, F. L. Meyskens Jr. and D. E. Brenner, *Cancer Prev. Res.*, 2011, **4**, 354–364.
9 M. Bayet-Robert, F. Kwiatkowski, M. Leheurteur, F. Gachon, E. Planchat, C. Abrial, M. A. Mouret-Reynier, X. Durando, C. Barthomeuf and P. Chollet, *Cancer Biol. Ther.*, 2010, **9**, 8–14.
10 H. Mirzaei, G. Naseri, R. Rezaee, M. Mohammadi, Z. Banikazemi, H. R. Mirzaei, H. Salehi, M. Peyvandi, J. M. Pawelek and A. Sahebkar, *Int. J. Cancer*, 2016, **139**, 1683–1695.
11 M. Mehanny, R. M. Hathout, A. S. Geneidi and S. Mansour, *J. Controlled Release*, 2016, **225**, 1–30.
12 R. Chang, L. Sun and T. J. Webster, *Int. J. Nanomed.*, 2014, **9**, 461–465.
13 S. Buss, J. Dobra, K. Goerg, S. Hoffmann, S. Kippenberger, R. Kaufmann, M. Hofmann and A. Bernd, *PLoS One*, 2013, **8**, e79748.
14 R. Pal, M. K. Mamidi, A. K. Das and R. Bhonde, *Arch. Toxicol.*, 2012, **86**, 651–661.
15 J. L. Hanslick, K. Lau, K. K. Noguchi, J. W. Olney, C. F. Zorumski, S. Mennerick and N. B. Farber, *Neurobiol. Dis.*, 2009, **34**, 1–10.
16 F. A. Oyarzun-Ampuero, G. R. Rivera-Rodriguez, M. J. Alonso and D. Torres, *Eur. J. Pharm. Sci.*, 2013, **49**, 483–490.
17 H. Rachmawati, D. K. Budiputra and R. Mauludin, *Drug Dev. Ind. Pharm.*, 2015, **41**, 560–566.
18 A. Kumar, A. Ahuja, J. Ali and S. Baboota, *Drug Delivery*, 2016, **23**, 214–229.
19 A. Prakash, R. Baskaran, N. Paramasivam and V. Vadivel, *Food Res. Int.*, 2018, **111**, 509–523.
20 F. Donsi and G. Ferrari, *J. Biotechnol.*, 2016, **233**, 106–120.
21 H. D. Silva, M. Â. Cerqueira and A. A. Vicente, *Food Bioprocess Technol.*, 2012, **5**, 854–867.
22 G. K. Jayaprakasha, L. Jagan Mohan Rao and K. K. Sakariah, *J. Agric. Food Chem.*, 2002, **50**, 3668–3672.
23 H. Urra, V. A. Torres, R. J. Ortiz, L. Lobos, M. I. Diaz, N. Diaz, S. Hartel, L. Leyton and A. F. Quest, *PLoS One*, 2012, **7**, e33085.
24 V. A. Torres, J. C. Tapia, D. A. Rodriguez, A. Lladser, C. Arredondo, L. Leyton and A. F. Quest, *Mol. Cell. Biol.*, 2007, **27**, 7703–7717.
25 C. Adura, S. Guerrero, E. Salas, L. Medel, A. Riveros, J. Mena, J. Arbiol, F. Albericio, E. Giralt and M. J. Kogan, *ACS Appl. Mater. Interfaces*, 2013, **5**, 4076–4085.
26 H. B. Chang, H. C. Huang, T. C. Huang, P. C. Yang, Y. Wang and H. F. Juan, *Bio-Protoc.*, 2013, **3**, e431.
27 L. Lobos-Gonzalez, L. Aguilar, J. Diaz, N. Diaz, H. Urra, V. A. Torres, V. Silva, C. Fitzpatrick, A. Lladser, K. S. Hoek, L. Leyton and A. F. Quest, *Pigm. Cell Melanoma Res.*, 2013, **26**, 555–570.
28 A. B. Alvero, D. Kim, E. Lima, N. J. Sumi, J. S. Lee, C. Cardenas, M. Pitruzzello, D. A. Silasi, N. Buza, T. Fahmy and G. Mor, *Sci. Rep.*, 2017, **7**, 40989.
29 E. Kinnear, L. J. Caproni and J. S. Tregoning, *PLoS One*, 2015, **10**, e0130375.
30 M. V. Lozano, G. Lollo, M. Alonso-Nocelo, J. Brea, A. Vidal, D. Torres and M. J. Alonso, *J. Nanopart. Res.*, 2013, **15**, 1515.
31 G. Lollo, P. Hervella, P. Calvo, P. Aviles, M. J. Guillen, M. Garcia-Fuentes, M. J. Alonso and D. Torres, *Int. J. Pharm.*, 2015, **483**, 212–219.
32 G. Lollo, G. R. Rivera-Rodriguez, J. Bejaud, T. Montier, C. Passirani, J. P. Benoit, M. Garcia-Fuentes, M. J. Alonso and D. Torres, *Eur. J. Pharm. Biopharm.*, 2014, **87**, 47–54.
33 G. R. Rivera-Rodriguez, G. Lollo, T. Montier, J. P. Benoit, C. Passirani, M. J. Alonso and D. Torres, *Int. J. Pharm.*, 2013, **458**, 83–89.
34 P. Agrawal, S. Soni, G. Mittal and A. Bhatnagar, *Int. J. Lower Extremity Wounds*, 2014, **13**, 180–190.
35 F. Croisier and C. Jérôme, *Eur. Polym. J.*, 2013, **49**, 780–792.
36 C. Danciu, A. Falamas, C. Dehelean, C. Soica, H. Radeke, L. Barbu-Tudoran, F. Bojin, S. C. Pinzaru and M. F. Munteanu, *Cancer Cell Int.*, 2013, **13**, 75.
37 M. A. Franco-Molina, D. F. Miranda-Hernandez, E. Mendoza-Gamboa, P. Zapata-Benavides, E. E. Coronado-Cerda, C. A. Sierra-Rivera, S. Saavedra-Alonso, R. S. Tamez-Guerra and C. Rodriguez-Padilla, *OncoTargets Ther.*, 2016, **9**, 243–253.
38 S. Anuchapreeda, Y. Fukumori, S. Okonogi and H. Ichikawa, *J. Nanotechnol.*, 2012, **2012**, 11.
39 C. Senft, M. Polacin, M. Priester, V. Seifert, D. Kogel and J. Weissenberger, *BMC Cancer*, 2010, **10**, 491.
40 S. Wang, S. Yu, W. Shi, L. Ge, X. Yu, J. Fan and J. Zhang, *IUBMB Life*, 2011, **63**, 775–782.
41 D. Bandyopadhyay, *Front. Chem.*, 2014, **2**, 113.
42 A. Hu, J. J. Huang, X. J. Jin, J. P. Li, Y. J. Tang, X. F. Huang, H. J. Cui, W. H. Xu and G. B. Sun, *Am. J. Cancer Res.*, 2015, **5**, 278–288.
43 C. L. Yang, Y. Y. Liu, Y. G. Ma, Y. X. Xue, D. G. Liu, Y. Ren, X. B. Liu, Y. Li and Z. Li, *PLoS One*, 2012, **7**, e37960.
44 L. I. Lin, Y. F. Ke, Y. C. Ko and J. K. Lin, *Oncology*, 1998, **55**, 349–353.
45 K. Chiablaem, K. Lirdprapamongkol, S. Keeratichamroen, R. Surarit and J. Svasti, *Anticancer Res.*, 2014, **34**, 1857–1864.
46 S. F. Hendrayani, H. H. Al-Khalaf and A. Aboussekhra, *Neoplasia*, 2013, **15**, 631–640.
47 Y. R. Ha, Y. W. Choi and S. J. Lee, *Food Sci. Biotechnol.*, 2011, **20**, 1615–1624.

48 H. I. Kim, H. Huang, S. Cheepala, S. Huang and J. Chung, *Cancer Prev. Res.*, 2008, **1**, 385–391.
49 S. S. Lin, K. C. Lai, S. C. Hsu, J. S. Yang, C. L. Kuo, J. P. Lin, Y. S. Ma, C. C. Wu and J. G. Chung, *Cancer Lett.*, 2009, **285**, 127–133.
50 J. Ravindran, S. Prasad and B. B. Aggarwal, *AAPS J.*, 2009, **11**, 495–510.
51 M. Lopez-Lazaro, *Mol. Nutr. Food Res.*, 2008, **52**(Suppl 1), S103–S127.
52 E. M. Jung, J. H. Lim, T. J. Lee, J. W. Park, K. S. Choi and T. K. Kwon, *Carcinogenesis*, 2005, **26**, 1905–1913.
53 L. Wang, Y. F. Li, L. Zhou, Y. Liu, L. Meng, K. Zhang, X. Wu, L. Zhang, B. Li and C. Chen, *Anal. Bioanal. Chem.*, 2010, **396**, 1105–1114.
54 D. Perrone, F. Ardito, G. Giannatempo, M. Dioguardi, G. Troiano, L. Lo Russo, A. De Lillo, L. Laino and L. Lo Muzio, *Exp. Ther. Med.*, 2015, **10**, 1615–1623.
55 S. Bhaumik, R. Anjum, N. Rangaraj, B. V. Pardhasaradhi and A. Khar, *FEBS Lett.*, 1999, **456**, 311–314.
56 J. H. Woo, Y. H. Kim, Y. J. Choi, D. G. Kim, K. S. Lee, J. H. Bae, D. S. Min, J. S. Chang, Y. J. Jeong, Y. H. Lee, J. W. Park and T. K. Kwon, *Carcinogenesis*, 2003, **24**, 1199–1208.
57 P. Javvadi, A. T. Segan, S. W. Tuttle and C. Koumenis, *Mol. Pharmacol.*, 2008, **73**, 1491–1501.
58 J. Cao, Y. Liu, L. Jia, H. M. Zhou, Y. Kong, G. Yang, L. P. Jiang, Q. J. Li and L. F. Zhong, *Free Radicals Biol. Med.*, 2007, **43**, 968–975.
59 Y. A. Larasati, N. Yoneda-Kato, I. Nakamae, T. Yokoyama, E. Meiyanto and J. Y. Kato, *Sci. Rep.*, 2018, **8**, 2039.
60 P. Calvo, J. L. Vila-Jato and M. J. Alonso, *J. Pharm. Sci.*, 1996, **85**, 530–536.
61 J. Crecente-Campo, S. Lorenzo-Abalde, A. Mora, J. Marzoa, N. Csaba, J. Blanco, A. Gonzalez-Fernandez and M. J. Alonso, *J. Controlled Release*, 2018, **286**, 20–32.
62 C. Teijeiro-Valino, E. Yebra-Pimentel, J. Guerra-Varela, N. Csaba, M. J. Alonso and L. Sanchez, *Nanomedicine*, 2017, **12**, 2069–2082.
63 G. R. Rivera-Rodriguez, M. J. Alonso and D. Torres, *Eur. J. Pharm. Biopharm.*, 2013, **85**, 481–487.
64 Z. Niu, I. Conejos-Sanchez, B. T. Griffin, C. M. O'Driscoll and M. J. Alonso, *Adv. Drug Delivery Rev.*, 2016, **106**, 337–354.
65 M. Norval, R. M. Lucas, A. P. Cullen, F. R. de Gruijl, J. Longstreth, Y. Takizawa and J. C. van der Leun, *Photochem. Photobiol. Sci.*, 2011, **10**, 199–225.
66 J. C. Becker, R. Houben, D. Schrama, H. Voigt, S. Ugurel and R. A. Reisfeld, *Exp. Dermatol.*, 2010, **19**, 157–164.
67 W. W. Overwijk and N. P. Restifo, *Curr. Protoc. Immunol.*, 2001, 1–33, ch. 20, unit 20.1.

